

RESEARCH

Open Access



Mutational spectrum associated with oculocutaneous albinism and Hermansky-Pudlak syndrome in nine Pakistani families

Jahangir Khan^{1,2}, Saaim Asif³, Shamsul Ghani¹, Hamid Khan¹, Muhammad Waqar Arshad⁴, Shujaat Ali Khan¹, Siying Lin⁵, Emma L. Baple⁵, Claire Salter⁵, Andrew H. Crosby⁵, Lettie Rawlins⁵ and Muhammad Imran Shabbir^{1*}

Abstract

Background Oculocutaneous albinism (OCA) is a genetically heterogeneous condition that is associated with reduced or absent melanin pigment in the skin, hair, and eyes, resulting in reduced vision, high sensitivity to light, and rapid and uncontrolled eye movements. To date, seventeen genes have been associated with OCA including syndromic and non-syndromic forms of the condition.

Methods Whole exome sequencing (WES) was performed to identify pathogenic variants in nine Pakistani families with OCA, with validation and segregation of candidate variants performed using Sanger sequencing. Furthermore, the pathogenicity of the identified variants was assessed using various *in-silico* tools and 3D protein structural analysis software.

Results WES identified biallelic variants in three genes explaining the OCA in these families, including four variants in *TYR*, three in *OCA2*, and two in *HPS1*, including two novel variants c.667C > T: p.(Gln223*) in *TYR*, and c.2009 T > C: p.(Leu670Pro) in *HPS1*.

Conclusions Overall, this study adds further knowledge of the genetic basis of OCA in Pakistani communities and facilitates improved management and counselling services for families suffering from severe genetic diseases in Pakistan.

Keywords *TYR*, *OCA2*, *HPS1*, Exome sequencing, Oculocutaneous albinism, Nystagmus, Pakistan

*Correspondence:

Muhammad Imran Shabbir
imran.shabbir@iiu.edu.pk

¹ Department of Biological Sciences, Faculty of Basic and Applied Sciences, International Islamic University, H-10, Islamabad 44000, Pakistan

² Faculty of Basic and Applied Sciences, SA-Centre for Interdisciplinary Research in Basic Sciences, International Islamic University, H-10, Islamabad 44000, Pakistan

³ Department of Biosciences, COMSATS University Islamabad, Islamabad Campus, Islamabad 45550, Pakistan

⁴ Department of Psychiatry, Yale University School of Medicine, VA CT Healthcare Center S116A2, West Haven 06516, USA

⁵ College of Medicine and Health, RILD Wellcome Wolfson Centre, University of Exeter, Royal Devon and Exeter NHS Foundation Trust, Barrack Road, Exeter EX2 5DW, UK



© The Author(s) 2024. **Open Access** This article is licensed under a Creative Commons Attribution-NonCommercial-NoDerivatives 4.0 International License, which permits any non-commercial use, sharing, distribution and reproduction in any medium or format, as long as you give appropriate credit to the original author(s) and the source, provide a link to the Creative Commons licence, and indicate if you modified the licensed material. You do not have permission under this licence to share adapted material derived from this article or parts of it. The images or other third party material in this article are included in the article's Creative Commons licence, unless indicated otherwise in a credit line to the material. If material is not included in the article's Creative Commons licence and your intended use is not permitted by statutory regulation or exceeds the permitted use, you will need to obtain permission directly from the copyright holder. To view a copy of this licence, visit <http://creativecommons.org/licenses/by-nc-nd/4.0/>.

Background

Albinism is a complex group of rare genetic disorders characterized by abnormal melanin biosynthesis, resulting in complete or partial loss of pigment (pheomelanin or eumelanin) with the addition of reduced visual acuity, photophobia (sensitivity to light), and nystagmus (random eye movements) [1]. It is divided into two major categories: ocular albinism (OA; MIM 300500), characterised by hypopigmentation of the ocular tissue, and oculocutaneous albinism (OCA; MIM 203100) (www.omim.org assessed on 30 January 2023) [2], which involves lack of pigmentation in the eyes, skin, and hair with nystagmus [3], misrouting of the optic nerves, foveal hypoplasia, and loss of vision. OCA is further classified into syndromic and non-syndromic forms. Non-syndromic OCA is caused by mutations in genes involved in melanin biosynthesis and melanocyte differentiation, resulting in only hypopigmentation and visual abnormalities [4]. Currently, seven genes (*TYR*, *OCA2*, *TYRP1*, *SLC45A2*, *SLC24A5*, *LRMDA*, and *DCT*) [5] linked to eight different types (OCA1-8) of non-syndromic OCA have been reported, with OCA1 being the most common, accounting for 50% of all cases reported worldwide associated with *TYR* gene variants [6]. Syndromic forms of OCA are associated with genes encoding proteins involved in the regulation of intercellular transport of molecules and the generation of lysosome-related organelles (LROs). LROs are specific to certain cell types, such as lytic granules in CD8+ T-cells and melanosomes in melanocytes. Disruption of this pathway can result in immunodeficiency, bleeding diathesis, and pulmonary fibrosis, as well as prominent OCA phenotypes such as hypopigmentation in the skin, eyes, and hair [7, 8]. Furthermore, syndromic OCA may include additional systemic changes. Hermansky-Pudlak syndrome (HPS; MIM 203300) and Chediak-Higashi syndrome (CHS; MIM 214500) are the two most common types of syndromic OCA. HPS is associated with mutations in genes involved in the formation of protein complexes (BLOC-1, BLOC-2, BLOC-3, or AP-3) and take part in biogenesis of specialized organelles such as melanosomes [9], whereas CHS is linked to mutations in the *LYST* gene located at *1q42-q43* and encodes a vascular transport protein whose function has not yet been fully delineated [10]. Clinical features of HPS generally include OCA with associated haematological problems (epistaxis, bleeding diathesis, menorrhagia, colonic and gingival bleeding and prolonged bleeding after surgery/trauma or postpartum hemorrhage), gastrointestinal anomalies (cramps, abdominal pain, enterocolitis, malabsorption, and diarrhoea), and respiratory issues (recurrent infection, exertional dyspnea, non-productive cough, pulmonary fibrosis, and hypoxia) [11]. To date, 11 HPS subtypes

associated with 11 different genes have been described in the literature. Both syndromic and non-syndromic OCA are inherited in an autosomal recessive pattern and have a global prevalence that ranges from 1: 17,000 to 20,000, with nearly one in every 70 individuals being a carrier [12, 13]. However, prevalence varies based on OCA type, ethnicity, and distinct founder mutations present in specific populations.

This study details the molecular genetic analysis of nine consanguineous Pakistani families from different ethnic backgrounds with OCA and signs of nystagmus. Whole exome sequencing (WES) identified nine pathogenic variants in three protein-coding genes, including two novel variants in the *TYR* and *HPS1* genes.

Methods

Ethical Approval

This study was approved by the International Islamic University's Institutional Review Board (IRB) in Islamabad, Pakistan (Letter No. IIU(BI&BT)/FBAS/2018/3598) and was carried out in accordance with the principles outlined in the Declaration of Helsinki. All participants in the study and/or their legal guardians provided written informed consent for clinical and research data to be published in a peer-reviewed journal. Nine affected families representing various ethnic groups were enrolled in this study from the Khyber Pakhtunkhwa (KPK) province of Pakistan. The clinical history of each family was recorded, and initial examination revealed the presence of OCA. Blood samples were collected from both affected and unaffected family members including their parents.

Clinical Examination

On initial analysis, complete family history and clinical information were obtained through questionnaire. The guardians of each of the families were interviewed about the onset of disease and all other related information. Pedigrees were constructed from information provided by the family using Cyrillic 2.0 software, according to the standard protocol defined by Bennett et al. (1995) [14]. After data collection, a detailed clinical evaluation was performed by a physician at the local district hospital for all affected and selected unaffected individuals from each of the nine families involved in the study to confirm their disease status. Colour vision analysis (Ishihara charts), visual acuity assessment (Snellen charts), photophobia, and fundoscopic examination by direct ophthalmoscopy were evaluated in affected individuals. Additionally, affected individuals were examined and assessed for pigment abnormalities in the skin, eyes, and hair to identify possible syndromic conditions associated with OCA.

Molecular genetic study

DNA was extracted from blood samples using an inorganic (salting out) protocol [15], carried out step by step at room temperature. Chemicals and reagents were kept at -4 °C and tightly sealed to avoid contamination. The NanoDrop™ spectrophotometer was used to determine the concentration and purity of the extracted DNA samples (Thermo Fisher Scientific, Dover, DE, USA).

WES was performed using an Illumina HiSeq™ 2000 sequencer on DNA from a single affected member from each of the nine families (Illumina Inc., San Diego, CA, USA). For exome enrichment, 51 Mb Agilent Sure Select Human All ExonV4 enrichment kit was used along with read alignment Burrows–Wheeler Aligner (BWA-MEM, v0.7.17) [16], InDel realignment, base quality recalibration Genome Analysis Tool Kit (GATK, v3.7.0) [17], SNVs/InDels (GATK/Haplotype Caller), duplicates removed and mate-pairs fixed using Picard (v2.15.0) (<http://broadinstitute.github.io/picard/>) and DNAnexus for annotation and variant calling (DNAnexus Inc., CA, USA: <https://dnanexus.com/>). Variant Call Format (VCF) files including all gene variations were generated using Haplotype Caller. Homozygosity was mapped using HomozygosityMapper [18]. The gnomAD database (<https://gnomad.broadinstitute.org/>) was used to detect allele frequencies, and GERP was used to conserve variants [19]. To identify candidate genes, single nucleotide polymorphisms (SNPs) with Minor Allele Frequency (MAF) (>0.05) were removed, along with non-splicing junctions containing synonymous and intronic variants found in the 1000 Genomes Project (www.1000genomes.org) [20] or the Single Nucleotide Polymorphism Database (dbSNP; NCBI).

Primers were designed using Primer3 software v0.4.0 (<http://frodo.wi.mit.edu/primer3/>) for all coding exons and associated intron–exon junctions of the *TYR* (NM_000372.5), *OCA2* (NM_000275.3), and *HPS1* (NM_000195.5) genes. To confirm co-segregation of the genetic variants identified by WES, PCR amplicons were generated in the Bio-Rad T100™ thermal cycler (Bio-Rad Laboratories, Hercules, CA, USA) using gene-specific primers (Supplementary Table 1) employing standard optimization procedures [21] and purified using the BIGDYE® X Terminator™ Purification Kit (ABI, Applied Biosystems, Waltham, MA, USA), with dideoxy sequencing of amplicons using an ABI 3730 DNA Analyzer (Thermo Fisher Scientific, Dover, DE, USA). Sequence reads were aligned to the human genome reference sequence [hg38] to identify base changes using BioEdit 7.0 (<http://www.mbio.ncsu.edu/BioEdit/bioedit.html>), CLC sequence viewer 8.0 (<http://www.clcbio.com/products/clc-sequence-viewer/>) and chromatograms visualized with FinchTV v1.5.0 (<https://digitallworldbiology.com/FinchTV>) software. Reference sequences for *TYR*, *OCA2*, and *HPS1* genes and proteins were obtained

from the Ensemble genome browser (GRCh38 assembly, Dec 2013) (http://www.ensembl.org/Homo_sapiens/Info/Index?db=core). Variant and allele frequencies were identified in ClinVar, HumVar, dbSNP, gnomAD v3.1.2, and HGMD 2022.1 online genomic databases, and the pathogenicity of *TYR*, *OCA2*, and *HPS1* gene variants was determined using the ACMG/AMP [22] guidelines.

Bioinformatics analysis

In silico pathogenicity prediction tools were used to assess missense and splice variants including REVEL (rare exome variant ensemble learner) [23] scores taken from dbNSFP (v4.3 a) (<http://database.liulab.science/dbNSFPconn>) [24], PredictSNP2 (<https://loschmidt.chemi.muni.cz/predictsnp2/>) [25], Scale-Invariant Feature Transform (SIFT) (<https://sift.bii.a-star.edu.sg/>) [26], Polymorphism phenotyping v2 (PolyPhen-2) (<http://genetics.bwh.harvard.edu/pph2/>) [27], Protein Variation Effect Analyzer (PROVEAN) (<https://www.jcvi.org/research/provean>) [28], SpliceAI (<https://spliceai.okup.broadinstitute.org/>) [29] and NNsplice (https://www.fruitfly.org/seq_tools/splice.html) [30].

Clustal Omega (<https://www.ebi.ac.uk/Tools/msa/clustalo/>) [31] was employed to show protein conservation across several species and for a three-dimensional (3D) structural analysis, the normal and mutant protein structures were generated using different protein prediction software's such as AlphaFold (<https://alphafold.ebi.ac.uk/>) [32], SWISS-MODEL (<https://swissmodel.expasy.org/>) [33], Phyre2 v2.0 (<http://www.sbg.bio.ic.ac.uk/~phyre2/>) [34], and RoseTTAFold (<https://robetta.bakerlab.org/>) [35]. Ramachandran plots were used to evaluate the stereochemistry and validity of the constructed 3D protein structures [36]. ERRAT [37], VERIFY 3D [38], WHATCHECK [39], and PROCHECK [36] evaluation tools (<https://saves.mbi.ucla.edu/>) were used for the assessment and verification of the predicted structures and then suitable structures were chosen based on their preferred regions and the ERRAT quality factor. Structures were analyzed using the Swiss-Pdb viewer (<https://spdbv.unil.ch/>) [40] to check for variant effect on protein structure. Furthermore, structure refinement, energy minimization, and visualization were done by UCSF Chimera 1.16 (<http://www.cgl.ucsf.edu/chimera>) [41].

Results

Clinical description

Nine consanguineous Pakistani families with OCA were recruited from Pakistan's KPK province. In all families, pedigree analysis revealed a recessive pattern of inheritance (Fig. 1). All affected individuals from the nine families showed signs of nystagmus and decreased visual acuity with depigmentation of the hair, eyes, and skin, whereas, the presence of photophobia, strabismus, colour blindness,

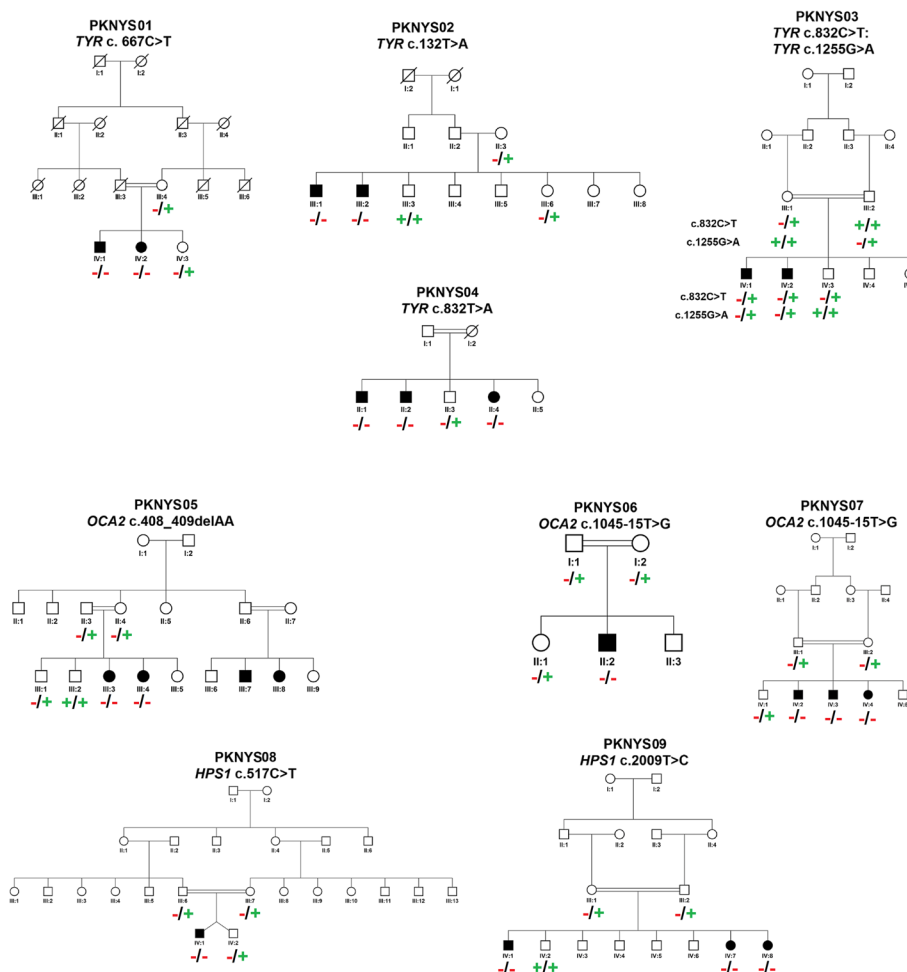


Fig. 1 Pedigrees of families. PKNYS (01–04) with OCA co-segregating for *TYR* mutations, PKNYS (05–07) with OCA co-segregating for *OCA2* mutations, and families PKNYS (08,09) with OCA co-segregating for *HPS1* mutations. “+” sign indicates wildtype allele whereas “-” sign indicates mutated allele. For compound heterozygous mutations, the different *TYR* variants within the same family are displayed in different colours

and foveal hypoplasia differed between individuals. In families PKNYS 08 and 09, additional symptoms of epistaxis, gingival bleeding, and bruising with severe and frequent respiratory infections were observed in affected individuals IV:1 from each family respectively, indicating the presence of a syndromic form of OCA (HPS). Detailed clinical evaluation is described in Table 1.

Genetic findings

Variants in *TYR*

WES identified four pathogenic *TYR* variants in families PKNYS (01–04), including a novel nonsense variant [Chr11(GRCh38):g.89178620C>T; NM_000372.5: c.667C>T; p.(Gln223*)] in the first exon of *TYR* in family PKNYS01, resulting in a premature termination codon (PTC) and truncated protein predicted to undergo nonsense-mediated decay (NMD). The MAF for the variant is not indexed in

gnomAD V3.1.2 and is listed as ‘pathogenic’ in ClinVar, however, there is no mention of zygosity. Furthermore, three previously reported [42–44] *TYR* variants were identified including a missense mutation in exon one [Chr11(GRCh38):g.89178085 T>A; NM_000372.5: c.132 T>A; p.(Ser44Arg)] in family PKNYS02, a nonsense mutation [Chr11(GRCh38):g.89191214C>T; NM_000372.5: c.832C>T; p.(Arg278*)] in family PKNYS03, and compound heterozygous variants in family PKNYS04 [NM_000372.5: Chr11(GRCh38):g.89191215C>T; c.832C>T; p.(Arg278*); and Chr11(GRCh38):g.89284843G>A; c.1255G>A; p.(Gly419Arg)] in exons one and four respectively. All variants co-segregated in families PKNYS 01–04 as expected for an autosomal recessive condition (see Fig. 1). All the identified variants were predicted to alter the function/expression of the *TYR* gene (Table 2).

Table 1 Clinical features observed in affected individuals with OCA

Family	PKNYS01	PKNYS02	PKNYS03	PKNYS04	PKNYS05	PKNYS06	PKNYS07	PKNYS08	PKNYS09
ID	IV:1	III:2	IV:2	II:1	III:3	II:2	IV:3	IV:1	IV:1
Age (Years)	40	8	14	7	6	4	4	16	10
Gender	Male	Male	Male	Male	Female	Male	Male	Male	Male
Province	KPK ^a	KPK ^a	KPK ^a	KPK ^a	KPK ^a	KPK ^a	KPK ^a	KPK ^a	KPK ^a
Caste	Niaz	Yousafzai	Afridi	Khattak	Afridi	Niaz	Yousafzai	Yousafzai	Khattak
Skin Colour	Reddish-White	Reddish-White	Reddish-White	White	White	White	White	White	Reddish-White
Hair Colour	White	White	White	White	White	White	White	White	White
Visual Acuity	LE 6/40	6/20	4/60	6/10	6/40	6/20	6/40	6/10	6/20
Iris Colour	RE Brown	6/40	4/60	6/10	6/20	6/20	6/40	6/20	6/10
		Light Grey/Blue	Violet/Reddish	Reddish	Light Grey/Blue	Light Grey/Blue	Light Grey/Blue	Light Grey/Blue	Reddish
Colour Blindness	Absent	Absent	Absent	Absent	Absent	Absent	Absent	Absent	Absent
Photophobia	Absent	Present	Present	Absent	Present	Present	Absent	NA	Present
Nystagmus	Present	Present	Present	Present	Present	Present	Present	Present	Present
Strabismus	NA	Absent	Present	Present	Absent	NA	Present	Absent	NA
Foveal Hypoplasia	Present	NA	Unable to determine	NA	Present	Unable to determine	NA	Present	Present
Fundus	Albinotic	Unable to determine	Albinotic	Albinotic	Unable to determine	NA	Unable to determine	Albinotic	Albinotic

Khyber Pakhtunkhwa^a

NA Not Available

Table 2 Variants observed in affected individuals with OCA

Family	PKNYS01	PKNYS02	PKNYS03	PKNYS04	PKNYS05	PKNYS06	PKNYS07	PKNYS08	PKNYS09
Gene	TYR	TYR	TYR	TYR	OCA2	OCA2	OCA2	HPS1	HPS1
Nucleotide Variant	c.667C>T	c.132T>A	c.832C>T; c.1255G>A	c.832C>T	c.408_409delAA	c.1045-15T>G	c.1045-15T>G	c.517C>T	c.2009T>C
Protein Variant	p.Gln223*	p.Ser44Arg	p.Arg278*; p.Gly419Arg	p.Arg278*	p.Arg137Ilefs*83	NA	NA	p.Arg173*	p.Leu670Pro
Status	Homozygous	Homozygous	Compound Heterozygous	Homozygous	Homozygous	Homozygous	Homozygous	Homozygous	Homozygous
Type of Mutation	Nonsense	Missense	Nonsense; Missense	Nonsense	Deletion	Splice site	Splice site	Nonsense	Missense
Previously Reported	Novel (This Study)	Yes [42]	Yes [43, 44]	Yes [43]	Yes [12]	Yes [45]	Yes [45]	Yes [46]	Novel (This Study)
ACMG Classification	Pathogenic (PVS1, PM2, PP3)	Pathogenic (PS4, PM1, PP2, PP3, PM2, PM3, PM5)	Pathogenic (PM2, PVS1 PP3, PP5); Pathogenic (PS4, PM2, PP1, PP3, PP4, PS3)	Pathogenic (PM2, PVS1, PP3, PP5)	Pathogenic (PP2, PM2, PVS1)	Pathogenic/ Likely pathogenic (PM1, PP2)	Pathogenic/ Likely pathogenic (PM1, PP2)	Pathogenic (PVS1, PM2, PP3, PP5)	Likely Pathogenic (PM1, PM2, BP1)
REVEL Score	-	0.840	-0.934	-	-	-	-	-	0.659
PredictSNP2	Del	Del	Unknown, Del	Unknown	-	Neutral	Neutral	Del	Del
SIFT	-	Dam	- Dam	-	-	-	-	-	Dam
PolyPhen-2	-	PD	- PD	-	-	-	-	-	PD
PROVEAN	-	Del	- Del	-	-	-	-	-	Del
SpliceAI	-	-	-	-	-	DL (0.00), AL (0.10)	DL (0.00), AL (0.10)	-	-
NNSPLICE	-	-	-	-	-	-0.4%	-0.4%	-	-
gnomAD v2.1.1 MAF	Absent	0.00001989	0.0001699 0.00006032	0.0001699	Absent	0.00002394	0.00002394	0.000004033	Absent
gnomAD v3.1.2 MAF	Absent	Absent	0.00008555 0.000006588	0.00008555	Absent	0.00001314	0.00001314	0.00002628	Absent
gnomAD v2.1.1 SA MAF	Absent	0	0.001274 0.0003921	0.001274	Absent	0.0001960	0.0001960	0	Absent
gnomAD v3.1.2 SA MAF	Absent	Absent	0.001452 0	0.001452	Absent	0.0004137	0.0004137	0	Absent

* Stop Codon, NA Not available, Dam Damaging, PD Probably damaging, Del/Deleterious, MAF Minor allele frequency, SA South Asian, DL Donor loss, AL Acceptor loss

Variants in *OCA2*

WES identified two previously reported variants [12, 45] in the *OCA2* gene in families PKNYS (05–07). The frameshift variant [Chr15(GRCh38):g.28027977_28027978DeTT; NM_000275.3: c.408_409delAA; p.(Arg137Ilefs*83)] located in exon four in family PKNYS05 and a splice site variant [Chr15(GRCh38):g.27990662A>C; NM_000275.3: c.1045-15 T>G; p.?] in families PKNYS 06 and 07 resulting in skipping of exon ten. All variants co-segregated as expected for an autosomal recessive condition in families PKNYS (05–07) (Fig. 1). The identified mutations are predicted to alter *OCA2* expression in the affected individuals resulting in the disease phenotype.

Variants in *HPS1*

WES identified one novel and one previously reported mutation in the *HPS1* gene in families PKNYS 08 and 09. The novel missense variant [Chr10(GRCh38):g.98417658A>G; NM_000195.5: c.2009 T>C; p.(Leu670Pro)] was located in exon twenty of *HPS1* in family PKNYS09. The MAF for the variant is not indexed in gnomAD V3.1.2 and is listed as 'likely pathogenic' in ClinVar, however, no clinical details are provided. The previously reported [46] nonsense mutation [Chr10(GRCh38):g.98431282G>A; NM_000195.5: c.517C>T; p.(Arg173*)] in exon seven in family PKNYS08. Co-segregation analysis in families PKNYS 08 and 09 revealed parents as heterozygous carriers and affected individuals as homozygous for these *HPS1* variants as expected for an autosomal recessive condition (Fig. 1).

In-Silico analysis

Various online tools were used to predict the pathogenicity of identified missense variants, including REVEL score, PredictSNP2, SIFT, PolyPhen-2, and PROVEAN. SpliceAI and NNSPLICE were used to assess the effect of splice variants. Table 2 details the results of these pathogenicity prediction tools alongside HGMD variant classification. SIFT, PolyPhen-2, PROVEAN, PredictSNP2, and Mutation Taster scores for the novel *HPS1* variant (NM_000195.5: c.2009 T>C; p.(Leu670Pro)) were 0.000, 0.998, -5.789, 1.000, and 0.999 respectively, and all predict the mutation to be deleterious.

Structural analysis

To investigate the effect and relationship between the wild-type (WT) and mutant protein structures for the novel *TYR* and *HPS1* variants, 3D-structural analysis was performed. It was predicted that the mutant *TYR* protein resulting from the nonsense variant (NM_000372.5: c.667C>T; p.Gln223*) would/may produce a truncated structure of only 222 amino acids in length (Fig. 2, Supplementary Fig. 1), caused by a PTC as compared to the

WT *TYR* protein comprising of 529 residues (Supplementary Fig. 1). Furthermore, Ramachandran plots of the WT *TYR* protein revealed 88.3% and 10.9% residues in the favored and allowed regions, while the mutant *TYR* protein consisting of only 222 amino acids (less than half of WT) had 88.9% and 11.9% residues in the favored and allowed regions (Supplementary Fig. 1). WT and mutant *TYR* structures were further analyzed in Swiss-Pdb viewer. The p. Gln223* termination was in the intra-melanosome domain of the *TYR* protein and resulted in a truncated non-functional protein structure. For the *HPS1* protein (700 residues), the missense variant (NM_000195.5: c.2009 T>C) was predicted to cause a substitution of amino acid leucine to proline at position 670 (Supplementary Fig. 2). The WT and mutant *HPS1* proteins were superimposed for direct comparison revealing conformational changes and altered quaternary structure of the mutant *HPS1* protein (Fig. 3C, D). Additionally, Ramachandran plots for the WT *HPS1* protein showed 87.8% and 11.2% residues in the favored and allowed regions, whereas the mutant *HPS1* protein had 87.6% and 11.9% residues in the favored and allowed regions (Supplementary Fig. 2). WT and mutant *HPS1* structures were then analyzed in Swiss-Pdb viewer. The p.Leu670Pro substitution was revealed to be located in C-terminal Fuz-longin-3 domain of the *HPS1* protein, which takes part in Rab signalling (Figs. 3 and 4) by forming a complex (BLOC-3) with *HPS3*. The substitution resulted in alteration of quaternary protein structure and predicted to disturb Rab signalling via BLOC-3. Overall, the reported pathogenic variants resulted in defective/ altered protein structures leading to the OCA phenotype in affected individuals.

Discussion

OCA is a clinically and genetically heterogeneous disorder that has been observed to segregate in an autosomal recessive pattern in humans [13]. This study identifies pathogenic variants in *TYR*, *OCA2*, and *HPS1* genes in affected individuals from nine Pakistani families with OCA (Table 1) portraying a recessive form of inheritance in all cases (Fig. 1). A total of nine mutations were identified using WES, including two novel variants in the *TYR* and *HPS1* genes (Table 2), moreover, *in-silico* analysis of altered amino acid sequences and 3D structural prediction further support the pathogenicity of these variants (Figs. 2, 3, 4 and Supplementary Fig. 1,2).

The *TYR* (NM_000372.5) gene located at chromosome 11q14.3 consists of five exons encoding an enzyme 523 amino acid residues in length which catalyzes the first two steps of the melanin biosynthesis pathway and involves oxidation and hydroxylation of

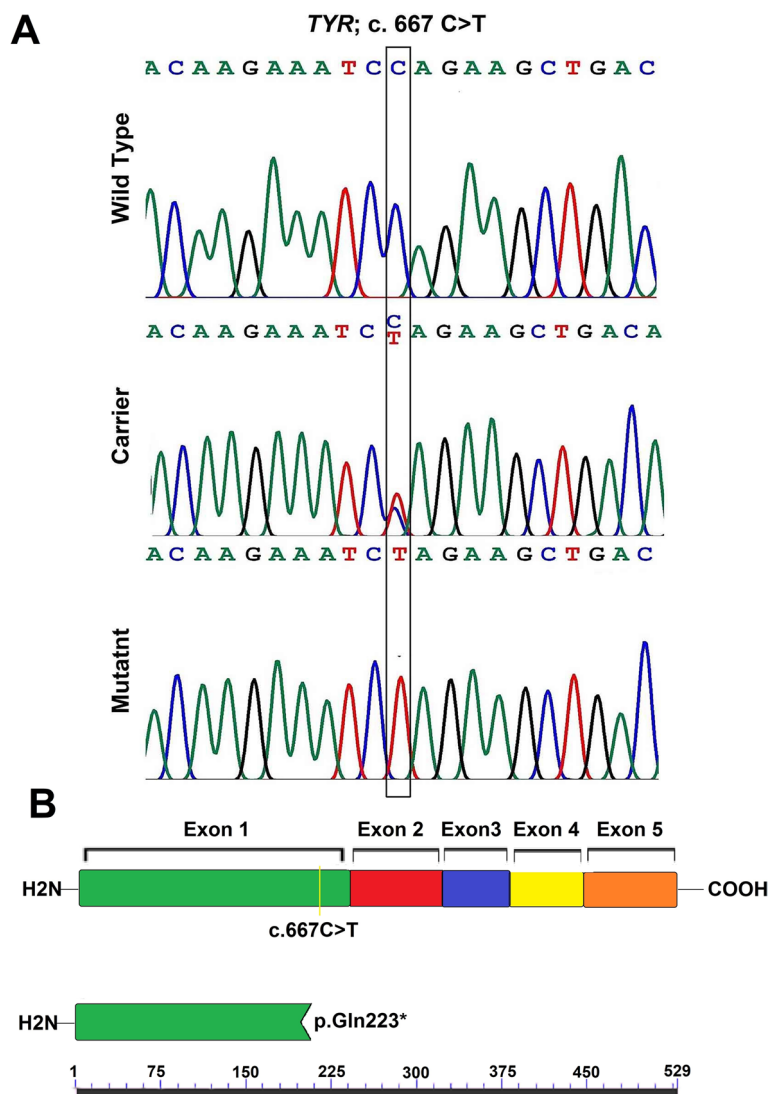


Fig. 2 Genetic analysis of family PKNYS01 with novel *TYR* variant. **A** From top to bottom: chromatograms of unaffected wildtype individual (Top), unaffected heterozygous carrier (Centre), and affected individual homozygous for thymine at position c.667. **B** Normal *TYR* structure consisting of five exons (1–5) which encode for the essential signal sequence, intra-melanosomal domain (consisting of epidermal growth factor (EGF)-like region and a Copper (Cu)-containing domains), and transmembrane-domain (Top); Mutated *TYR* structure showing stop codon at position p. Gln 223* in the intra-melanosomal domain along with scale for amino acid length (Bottom)

L-DOPA and DOPA quinone. The glycoprotein structure consists of four regions, a signal sequence (1-18), an intra-melanosomal domain (19-476) comprising of a copper binding site, a single α -helical trans-membrane domain (477-497), and a flexible C-terminal domain (498-529) [49]. To date, over 565 pathogenic variants have been reported in the *TYR* gene (HGMD 2022.1) (Table 3) with over 90 mutations identified in the Pakistani population, accounting for 40% of OCA cases. Furthermore, the prevalence of *TYR* allele in the Pakistani population accounts for about 37% [50]. In families PKNYS (01–04) four mutations (three previously

reported, one novel) were identified in the *TYR* gene. Among the reported variants, c.132 T > A (p.Ser44Arg) has been previously described in three Pakistani families and is more common in the South Asian population according to gnomAD v2.1.2 MAF (0.0013), compared to other populations (African 0.0001249, and European 0.00002372) [51]. The *TYR* variants (p.Gly419Arg) c.1255G > A and (p.Arg278*) c.832C > T are amongst the most frequently reported mutations in the Pakistani community occurring in 20 and 21 families, respectively [5]. The reported nonsense/mis-sense variants c.132 T > A, c.832C > T and c.1255G > A

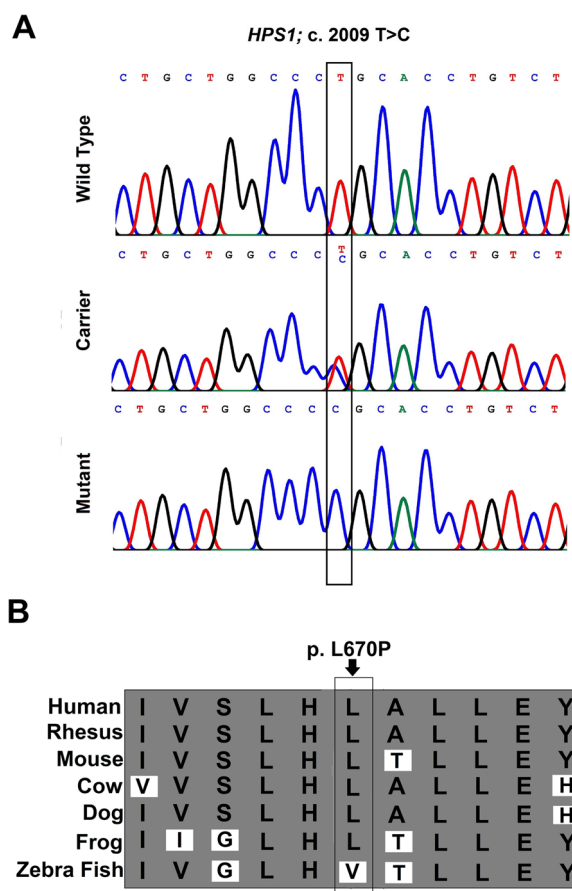


Fig. 3 Genetic analysis of family PKNYS09 with novel *HPS1* variant. **A** From top to bottom: chromatograms of unaffected wildtype individual (Top), unaffected heterozygous carrier (Centre), and affected individual homozygous for cytosine at position c.2009. **B** ClustalO multiple amino acid sequence alignment of *HPS1* orthologs shows p.Leu670 as highly conserved among species (shaded area represent conserved amino acids; light area represent non-conserved amino acids)

(p.Ser44Arg, p.Arg278* and p.Gly419Arg) were found to be rare with MAF 0.0001, 0.0001, and 0.00006 worldwide respectively [50] whereas, MAF for the novel *TYR* nonsense variant c.667C>T (p.Gln223*) was not listed in gnomAD v3.1.2. The c.667C>T; p.(Gln223*) variant is listed as pathogenic in ClinVar, although there are limited clinical details and no information on zygosity. The variant results in a truncated non-functional structure occurring in the first exon encoding the intramelanosomal domain (IMD) (conserved region), which facilitate the enzymatic conversion of the amino acid tyrosine into melanin. The IMD of tyrosinase contains the active site of the enzyme, where it catalyzes two key reactions in the melanin synthesis pathway: (1) Hydroxylation of Tyrosine and (2) Oxidation of DOPA. These enzymatic reactions are crucial in melanin

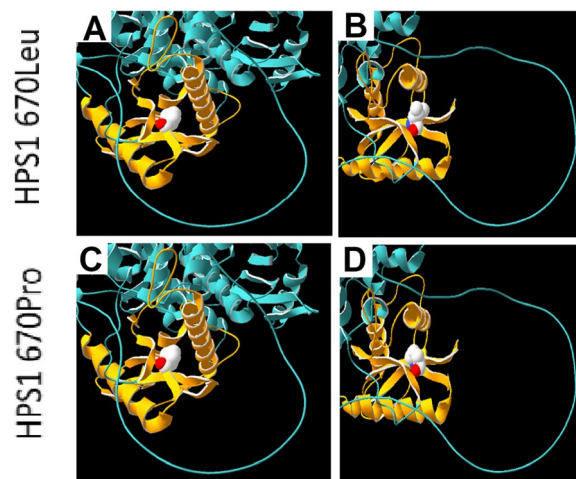


Fig. 4 Protein modelling studies (Swiss model, SPDBV v4.10) demonstrating the location of the *HPS1* 670Leu position within the C-terminal Fuz-longin-3 domain (Third Longin domain of FUZ, MON1 and *HPS1*, orange) [47, 48]. Structurally this domain is composed of an α/β fold which contains five anti-parallel β -strands organised as a central β -sheet, with two α -helices around it (Sanchez-Pulido & Ponting, 2020). **(A, B)** demonstrate the reference amino acid Leucine and **(C, D)** show the alternate Proline arising from the novel *HPS1* variant (NM_000195.5: c.2009 T>C; p.(Leu670Pro)). The location of this variant within the central β -sheet is likely to affect the function of this domain in Rab signalling

Table 3 Genes associated with non-syndromic OCA

Locus	Genes	Number of variants listed in HGMD	Identified in number of Pakistani families
OCA1	<i>TYR</i>	565	100+
OCA2	<i>OCA2</i>	431	59
OCA3	<i>TYRP1</i>	63	10+
OCA4	<i>SLC45A2</i>	207	10+
OCA6	<i>SLC24A5</i>	35	3
OCA7	<i>LRMDA</i>	6	-
OCA8	<i>DCT</i>	6	-

biosynthesis. Alterations in the IMD results in loss of *TYR* function leading to genetic conditions such as OCA [52] like in family PKNYS01. In families PKNYS (05–07) two previously reported mutations were identified in the *OCA2* gene responsible for OCA type 2 (second most prevalent form of OCA), which has a global prevalence of 1 in 36,000. The *OCA2* (NM_000275.3) gene previously known as the ‘P’ gene is composed of 23 exons and codes for a melanosomal transmembrane enzyme consisting of 838 residues (10 kDa) [53]. Until now, more than 431 mutations have been reported in the *OCA2* gene (HGMD 2022.1) (Table 3), with a total of 59 variants reported in the Pakistani population in

seven studies. MAF for the identified *OCA2* mutations c.408_409delAA (p.Arg137Ilefs*83) and c.1045-15 T>G (splice site mutation) in families PKNYS (05, and 06/07) shows not listed and 0.00002 respectively in gnomAD v3.1.2 [51]. The splice site variant c.1045-15 T>G although very rare has been widely reported in more than 17 families belonging to the Pakistani population accounting for over 30% of the total mutations in the *OCA2* gene [50] whereas, the frameshift variant c.408_409delAA (p.Arg137Ilefs*83) identified in family PKNYS05 has only been reported once before in a single Pakistani family [12].

In addition to the OCA phenotype, the affected individuals (IV:1) from families PKNYS 08 and 09 showed symptoms like epistaxis and bruising accompanied by infections, indicating the presence of HPS (syndromic OCA). WES identified one novel and one previously reported variant in the *HPS1* gene in affected individuals. The *HPS1* (NM_000195.5) gene responsible for HPS type 1 is located on the reverse strand of chromosome 10q23.1-q23.3 and codes for a 700-residue protein structure [54], which plays a crucial role in melanosome regulation, organelle biogenesis, and has been reported to interact with TYR, TYRP1 and TRP2/DCT. *HPS1* affects individuals of different ethnicities, including those from European, Asian, and South American backgrounds. It has a global prevalence of 1/1,500,000–1,000,000, although the prevalence is 1/1800 in individuals of Puerto Rican descent [55]. Over 98 mutations have been reported in the *HPS1* gene (HGMD 2022.1), with 9 variants identified in the Pakistani population in four reports [11] from all HPS subtypes, of which three mutations were present in the *HPS1* gene (c.1342 T>C, genomic deletion, c.2056C>T) [56]. The reported variant c.517C>T (p.Arg173*) in family PKNYS08 has been previously described in the Chinese population [46] and although is rare with a MAF of 0.00003, whereas the MAF for the novel mutation c.2009 T>C (p.Leu670Pro) is not listed in gnomAD v3.1.2, and this variant is listed as likely pathogenic in Clinvar, although no evidence or clinical details are provided. The variant lies in the C-terminal Fuz-longin-3 domain (conserved region; Figs. 3 and 4) of the *HPS1* protein which forms a complex (BLOC-3) with *HPS4*. This complex acts as a guanine nucleotide exchange factor (GEF) and shows specific activity toward Ra32/38 and can promote recruitment of Rab32 and Rab38 to membrane. Furthermore, BLOC-3 and its target Rabs act in the biogenesis of melanosomes and alterations in these complexes have been reported to cause syndromic forms of OCA like HPS [47, 48]. The resulting substitution p.Leu670Pro induces changes in the fuzz-domain of *HPS1* protein altering the quaternary structure due to different characteristics of the amino acids leading to changes in Rab signalling (Fig. 4)

thus, supporting the pathogenicity of this variant in family PKNYS09. Currently, there is no potential treatment for OCA, and management strategies focus on proper eye care and monitoring skin for problems.

Conclusion

Our study identifies novel and reported variants in the *TYR*, *OCA2*, and *HPS1* genes and broadens the mutational spectrum and genetic heterogeneity of OCA in the Pakistani population. We further predict the deleterious outcome of novel variants using *in-silico* variant prediction tools and structural analysis. These findings will assist in providing an early diagnosis for affected individuals and facilitate the provision of possible genetic counselling for affected families in the Pakistani community and worldwide.

Supplementary Information

The online version contains supplementary material available at <https://doi.org/10.1186/s12886-024-03611-6>.

Supplementary Material 1. Supplementary Figure 1 3D structure of TYR protein. (A) wild type TYR from UniProt ID: P14679. (B) mutant TYR truncated at p. Q223* predicted using RoseTTAFold (C) Ramachandran plot of wild type TYR protein model (D) Ramachandran plot of Q223* mutant TYR protein structure.

Supplementary Material 2. Supplementary Figure 2 Superimposed 3D structure. (A) Wild type *HPS1* (light blue) from UniProt ID: Q92902 and mutant *HPS1* (purple) predicted using RoseTTAFold (B) Analysis of wildtype and mutant *HPS1* proteins: (left) normal *HPS1* structure depicting Leu670 in yellow; (right) altered *HPS1* protein showing Pro670 substitution in red (C) Ramachandran plot of wild type *HPS1* protein structure (D) Ramachandran plot of L670P mutant *HPS1* protein model.

Supplementary Material 3. Supplementary Table 1 List of specific primer sequences for *TYR*, *OCA2*, and *HPS1* genes used for co-segregation analysis in families with OCA.

Acknowledgements

We are thankful to all the individuals and their families for participating in this study. We also thank all clinicians and geneticists that helped us to perform this study in any shape specially Lyton-Rehmatullah Benevolent Trust (LRBT), and Christian Hospital, Quetta, Pakistan.

Authors' contributions

Conceptualization, J.K and M.I.S; methodology, J.K, S.G, H.K, S.A.K and M.W.A; software, S.A and M.I.S; validation, S.A; formal analysis, J.K; investigation, J.K, C.G.S and S.L; resources, M.I.S, E.L.B, and A.H.C; data curation, J.K, S.A, L.E.R and M.I.S; writing—original draft preparation, J.K, S.A and M.I.S; writing—review and editing All Authors; supervision, E.L.B, A.H.C and M.I.S; project administration, M.I.S; funding acquisition, E.L.B and A.H.C; All authors have read and approved the final version of the manuscript.

Authors information

Not applicable.

Funding

This study was partially supported by the Higher Education Commission (HEC) of Pakistan by awarding International Research Support Initiative Program (IRSIP) (Grant No: 1–8/HEC/HRD/2017/8347, PIN: IRSIP 39 BMS 1) to J.K and RILD Wellcome Wolfson Centre (Level 4), Royal Devon and Exeter NHS Foundation Trust, UK. Exome/Sanger sequencing and analysis was carried out at RILD Wellcome Wolfson Center UK and was funded by HEC Pakistan and Wellcome Trust UK (to E.L.B).

Availability of data and materials

The patient's non-sensitive datasets used and/or analysed during the current study are available from the corresponding authors on reasonable request.

Declarations**Ethics approval and consent to participate**

The study was approved by the Institutional Review Board (IRB) of the International Islamic University, Islamabad, Pakistan (Letter No. IIU(BI&BT)/FBAS/2018/3598), and the study was carried out in accordance with the principles outlined in the Declaration of Helsinki. Written informed consent were obtained from individuals > 18 years and from parents/guardians of individuals < 18 year participated in this study.

Consent for publication

Not Applicable.

Competing interests

The authors declare no competing interests.

Received: 29 June 2023 Accepted: 20 November 2023

Published online: 14 August 2024

References

- Shah S, Saeed A, Irshad M, Babar M, Hussain T. Oculocutaneous albinism in Pakistan: A review. *J Cancer Sci Ther*. 2018;10:253–7.
- Rocca C, Tiberi L, Bargiacchi S, Palazzo V, Landini S, Marziali E, Caputo R, Tinelli F, Marchi V, Benedetto A. Expanding the Spectrum of Oculocutaneous Albinism: Does Isolated Foveal Hypoplasia Really Exist? *Int J Mol Sci*. 2022;23:7825.
- Arshad MW, Shabbir MI, Asif S, Shahzad M, Leydier L, Rai SK. FRMD7 Gene Alterations in a Pakistani Family Associated with Congenital Idiopathic Nystagmus. *Genes*. 2023;14(2):346.
- Schidlowski L, Liebert F, Iankilevich PG, Rebellato PRO, Rocha RA, Almeida NAP, Jain A, Wu Y, Itan Y, Rosati R. Non-syndromic oculocutaneous albinism: novel genetic variants and clinical follow up of a brazilian pediatric cohort. *Front Genet*. 2020;11:397.
- Ullah MI. Clinical and Mutation Spectrum of Autosomal Recessive Non-Syndromic Oculocutaneous Albinism (nsOCA) in Pakistan: A Review. *Genes*. 2022;13:1072.
- Shakil M, Akbar A, Aisha NM, Hussain I, Ullah MI, Atif M, Kaul H, Amar A, Latif MZ, Qureshi MA. Delineating Novel and Known Pathogenic Variants in TYR, OCA2 and HPS-1 Genes in Eight Oculocutaneous Albinism (OCA) Pakistani Families. *Genes*. 2022;13:503.
- Fernández A, Hayashi M, Garrido G, Montero A, Guardia A, Suzuki T, Montoliu L. Genetics of non-syndromic and syndromic oculocutaneous albinism in human and mouse. *Pigment Cell Melanoma Res*. 2021;34:786–99.
- Bibi N, Ullah A, Darwesh L, Khan W, Khan T, Ullah K, Khan B, Ahmad W, Umm-e-Kalsoom. Identification and computational analysis of novel tyr and slc45a2 gene mutations in Pakistani families with identical non-syndromic oculocutaneous Albinism. *Front Genet*. 2020;11:749.
- El-Chemaly S, Young LR. Hermansky-pudlak syndrome. *Clin Chest Med*. 2016;37:505–11.
- Ajitkumar A, Yarrarapu SNS, Ramphul K. Chediak Higashi Syndrome. 2018.
- Zaman Q, Anas M, Rehman G, Khan Q, Iftikhar A, Ahmad M, Owais M, Ahmad I, Muthaffar OY, Abdulkareem AA. Report of Hermansky-Pudlak Syndrome in Two Families with Novel Variants in HPS3 and HPS4 Genes. *Genes*. 2023;14:145.
- Arshad MW, Harlalka GV, Lin S, D'Atri I, Mehmood S, Shakil M, Hassan MJ, Chioza BA, Self JE, Ennis S. Mutations in TYR and OCA2 associated with oculocutaneous albinism in Pakistani families. *Meta Gene*. 2018;17:48–55.
- Sajid Z, Yousaf S, Waryah YM, Mughal TA, Kausar T, Shahzad M, Rao AR, Abbasi AA, Shaikh RS, Waryah AM. Genetic causes of oculocutaneous albinism in Pakistani population. *Genes*. 2021;12:492.
- Bennett RL, Steinhaus KA, Uhrich SB, O'Sullivan CK, Resta RG, Lochner-Doyle D, Markel DS, Vincent V, Hamanishi J. Recommendations for standardized human pedigree nomenclature. *J Genet Couns*. 1995;4:267–79.
- Grimberg J, Nawoschik S, Belluscio L, McKee R, Turck A, Eisenberg A. A simple and efficient non-organic procedure for the isolation of genomic DNA from blood. *Nucleic Acids Res*. 1989;17:8390.
- Li H, Durbin R. Fast and accurate short read alignment with Burrows-Wheeler transform. *Bioinformatics*. 2009;25:1754–60.
- McKenna A, Hanna M, Banks E, Sivachenko A, Cibulskis K, Kernytsky A, Garimella K, Altshuler D, Gabriel S, Daly M. The Genome Analysis Toolkit: a MapReduce framework for analyzing next-generation DNA sequencing data. *Genome Res*. 2010;20:1297–303.
- Seelow D, Schuelke M, Hildebrandt F, Nürnberg P. HomozygosityMapper—an interactive approach to homozygosity mapping. *Nucleic acids research*. 2009;37(suppl_2):W593–9.
- Davydov EV, Goode DL, Sirota M, Cooper GM, Sidow A, Batzoglou S. Identifying a high fraction of the human genome to be under selective constraint using GERP++. *PLoS computational biology*. 2010;6(12):e1001025.
- Karczewski KJ, Francioli LC, Tiao G, Cummings BB, Alfoldi J, Wang Q, MacArthur DG, et al. The mutational constraint spectrum quantified from variation in 141,456 humans. *Nature*. 2020;581(7809):434–43.
- Asif S, Khan M, Arshad MW, Shabbir MI. PCR Optimization for Beginners: A Step by Step Guide. *Research in Molecular Medicine*. 2021;9:81–102. <https://doi.org/10.32598/rmm.9.2.1189.1>.
- Richards S, Aziz N, Bale S, Bick D, Das S, Gastier-Foster J, Grody WW, Hegde M, Lyon E, Spector E. Standards and guidelines for the interpretation of sequence variants: a joint consensus recommendation of the American College of Medical Genetics and Genomics and the Association for Molecular Pathology. *Genet Med*. 2015;17:405–23.
- Ioannidis NM, Rothstein JH, Pejaver V, Middha S, McDonnell SK, Baheti S, Musolf A, Li Q, Holzinger E, Karyadi D. REVEL: an ensemble method for predicting the pathogenicity of rare missense variants. *The American Journal of Human Genetics*. 2016;99:877–85.
- Liu X, Li C, Mou C, Dong Y, Tu Y. dbNSFP v4: a comprehensive database of transcript-specific functional predictions and annotations for human nonsynonymous and splice-site SNVs. *Genome medicine*. 2020;12:1–8.
- Bendl J, Musil M, Štourač J, Zendluka J, Damborský J, Brezovský J. PredictSNP2: a unified platform for accurately evaluating SNP effects by exploiting the different characteristics of variants in distinct genomic regions. *PLoS Comput Biol*. 2016;12: e1004962.
- Lowe DG. Object recognition from local scale-invariant features. In: Proceedings of the Proceedings of the seventh IEEE international conference on computer vision. 1999. p. 1150–7.
- Adzhubei IA, Schmidt S, Peshkin L, Ramensky VE, Gerasimova A, Bork P, Kondrashov AS, Sunyaev SR. A method and server for predicting damaging missense mutations. *Nat Methods*. 2010;7:248–9.
- Choi Y, Chan AP. PROVEAN web server: a tool to predict the functional effect of amino acid substitutions and indels. *Bioinformatics*. 2015;31:2745–7.
- Jaganathan K, Panagiotopoulou SK, McRae JF, Darbandi SF, Knowles D, Li YI, Kosmicki JA, Arbelaez J, Cui W, Schwartz GB. Predicting splicing from primary sequence with deep learning. *Cell*. 2019;176(535–548): e524.
- Reese MG, Eeckman FH, Kulp D, Haussler D. Improved splice site detection in Genie. In: Proceedings of the Proceedings of the first annual international conference on Computational molecular biology. 1997. p. 232–40.
- Larkin MA, Blackshields G, Brown NP, Chenna R, McGettigan PA, McWilliam H, Valentin F, Wallace IM, Wilm A, Lopez R. Clustal W and Clustal X version 2.0. *Bioinformatics*. 2007;23:2947–8.
- Jumper J, Evans R, Pritzel A, Green T, Figurnov M, Ronneberger O, Tunyasuvunakool K, Bates R, Židek A, Potapenko A. Highly accurate protein structure prediction with AlphaFold. *Nature*. 2021;596:583–9.
- Waterhouse A, Bertoni M, Bienert S, Studer G, Tauriello G, Gumienny R, Heer FT, de Beer TAP, Rempfer C, Bordoli L. SWISS-MODEL: homology modelling of protein structures and complexes. *Nucleic Acids Res*. 2018;46:W296–303.
- Kelley LA, Mezulis S, Yates CM, Wass MN, Sternberg MJ. The Phyre2 web portal for protein modeling, prediction and analysis. *Nat Protoc*. 2015;10:845–58.
- Baek M, DiMaio F, Anishchenko I, Dauparas J, Ovchinnikov S, Lee GR, Wang J, Cong Q, Kinch LN, Schaeffer RD. Accurate prediction of protein structures and interactions using a three-track neural network. *Science*. 2021;373:871–6.

36. Laskowski RA, MacArthur MW, Moss DS, Thornton JM. PROCHECK: a program to check the stereochemical quality of protein structures. *J Appl Crystallogr.* 1993;26:283–91.
37. Colovos C, Yeates TO. Verification of protein structures: patterns of non-bonded atomic interactions. *Protein Sci.* 1993;2:1511–9.
38. Lüthy R, Bowie JU, Eisenberg D. Assessment of protein models with three-dimensional profiles. *Nature.* 1992;356:83–5.
39. Hoofst RW, Vriend G, Sander C, Abola EE. Errors in protein structures. *Nature.* 1996;381:272–272.
40. Guex N, Peitsch MC. SWISS-MODEL and the Swiss-Pdb Viewer: an environment for comparative protein modeling. *Electrophoresis.* 1997;18(15):2714–23.
41. Pettersen EF, Goddard TD, Huang CC, Couch GS, Greenblatt DM, Meng EC, Ferrin TE. UCSF Chimera—a visualization system for exploratory research and analysis. *J Comput Chem.* 2004;25:1605–12.
42. Shah S, Raheem N, Daud S, Mubeen J, Shaikh A, Baloch A, Nadeem A, Tayyab M, Babar M, Ahmad J. Mutational spectrum of the TYR and SLC45A2 genes in Pakistani families with oculocutaneous albinism, and potential founder effect of missense substitution (p. Arg77Gln) of tyrosinase. *Clin Exp Dermatol.* 2015;40:774–80.
43. Wang X, Zhu Y, Shen N, Peng J, Wang C, Liu H, Lu Y. Mutation analysis of a Chinese family with oculocutaneous albinism. *Oncotarget.* 2016;7:84981.
44. Chaki M, Sengupta M, Mondal M, Bhattacharya A, Mallick S, Ray K. Molecular and functional studies of tyrosinase variants among Indian oculocutaneous albinism type 1 patients. *Differentiation.* 2011;22:2992–3003.
45. Jaworek TJ, Kausar T, Bell SM, Tariq N, Maqsood MI, Sohail A, Ali M, Iqbal F, Rasool S, Riazuddin S. Molecular genetic studies and delineation of the oculocutaneous albinism phenotype in the Pakistani population. *Orphanet J Rare Dis.* 2012;7:1–19.
46. Wei A, Yuan Y, Bai D, Ma J, Hao Z, Zhang Y, Yu J, Zhou Z, Yang L, Yang X. NGS-based 100-gene panel of hypopigmentation identifies mutations in Chinese Hermansky-Pudlak syndrome patients. *Pigment Cell Melanoma Res.* 2016;29:702–6.
47. Gerondopoulos A, Langemeyer L, Liang J-R, Linford A, Barr FA. BLOC-3 mutated in Hermansky-Pudlak syndrome is a Rab32/38 guanine nucleotide exchange factor. *Curr Biol.* 2012;22(22):2135–9.
48. Sanchez-Pulido L, Ponting CP. Hexa-Longin domain scaffolds for inter-Rab signalling. *Bioinformatics.* 2020;36(4):990–3.
49. Sun W, Shen Y, Shan S, Han L, Li Y, Zhou Z, Zhong Z, Chen J. Identification of TYR mutations in patients with oculocutaneous albinism. *Mol Med Rep.* 2018;17:8409–13.
50. Shakil M, Harlalka GV, Ali S, Lin S, D'Atri I, Hussain S, Nasir A, Shahzad MA, Ullah MI, Self JE. Tyrosinase (TYR) gene sequencing and literature review reveals recurrent mutations and multiple population founder gene mutations as causative of oculocutaneous albinism (OCA) in Pakistani families. *Eye.* 2019;33:1339–46.
51. Shahzad M, Yousaf S, Waryah YM, Gul H, Kausar T, Tariq N, Mahmood U, Ali M, Khan MA, Waryah AM. Molecular outcomes, clinical consequences, and genetic diagnosis of Oculocutaneous Albinism in Pakistani population. *Sci Rep.* 2017;7:44185.
52. Farney SK, Dolinska MB, Sergeev YV. Dynamic analysis of human tyrosinase intra-melanosomal domain and mutant variants to further understand oculocutaneous albinism type 1. *Journal of analytical & pharmaceutical research.* 2018;7(6):621.
53. Donnelly MP, Paschou P, Grigorenko E, Gurwitz D, Barta C, Lu R-B, Zhukova OV, Kim J-J, Siniscalco M, New M. A global view of the OCA2-HERC2 region and pigmentation. *Hum Genet.* 2012;131:683–96.
54. Huizing M, Malicdan MCV, Gochuico BR, Gahl WA. Hermansky-pudlak syndrome. 2021.
55. Rojas WDJ, Young LR. Hermansky–Pudlak syndrome. In: *Proceedings of the Seminars in Respiratory and Critical Care Medicine.* 2020. p. 238–46.
56. Yousaf S, Shahzad M, Tasleem K, Sheikh SA, Tariq N, Shabbir AS, Ali M, Waryah AM, Shaikh RS, Riazuddin S. Identification and clinical characterization of Hermansky-Pudlak syndrome alleles in the Pakistani population. *Pigment Cell Melanoma Res.* 2016;29:231.

Publisher's Note

Springer Nature remains neutral with regard to jurisdictional claims in published maps and institutional affiliations.